Bulletin of the Geological Society of Malaysia, Volume 82, November 2026, pp. 45 - 58
DOI: https://doi.org/10.7186/bgsm82202605

Mapping the seismic vulnerability index: A case study of Kajai Village, West Pasaman Regency, Indonesia

Adree Octova[1,2], Muhammad Irman Khalif Ahmad Aminuddin[2,*], Harizona Aulia Rahman[3], Dedi Yulhendra[1], Aulia Hidayat Burhamidar[3], Yoszi Mingsi Anaperta[1], Riko Maiyudi[1], Mulya Gusman[1], Silvia Suryanita[1]

[1] Department of Mining Engineering, Universitas Negeri Padang, Prof Hamka Street, Padang 25131, Indonesia
[1,2] School of Materials and Mineral Resources Engineering, Universiti Sains Malaysia, Nibong Tebal, Penang 14300, Malaysia
[3] Department of Geological Engineering, Universitas Negeri Padang, Prof. Hamka Street, Padang 25131, Indonesia
* Corresponding author email address: irmankhalif@usm.my

Abstract: West Sumatra is highly susceptible to earthquakes due to its position near the convergent boundary of the Indo-Australian and Eurasian plates, encompassing major seismic zones such as the Megathrust, Mentawai Fault, and Sumatra Fault. On February 25, 2022, a magnitude 6.2 earthquake struck near Mount Talamau, causing significant damage in Kajai Village, Talamau District, West Pasaman Regency. This event highlighted the need for a detailed assessment of the area's seismic vulnerability. To address this, seismic vulnerability index mapping was carried out using microtremor measurements, analyzed through the Horizontal-to-Vertical Spectral Ratio (HVSR) method. Dominant frequency and amplification factors were calculated to evaluate the area's susceptibility to seismic damage. Dominant frequencies in the study area range from 0.66 Hz to 12.58 Hz, with lower frequencies indicating thick, soft sediment layers. Amplification factors range from 2.95 to 8.50, reflecting varying levels of seismic wave amplification. Based on these parameters, the seismic vulnerability index classifies the area into low, medium, and high vulnerability zones. High-vulnerability zones, defined by index values exceeding 20×10^{-6} s²/cm, are primarily concentrated near the Talamau Fault. These areas are characterized by low dominant frequencies and high amplification factors, indicating a heightened potential for severe seismic impacts. The findings underscore the need for targeted mitigation measures, such as structural reinforcements and improved disaster preparedness, especially in high-risk zones. This study provides critical data to support future seismic risk assessments and the formulation of effective earthquake mitigation strategies.

Keywords: Seismic vulnerability index, HVSR, mapping, microtremors, Kajai Village, Indonesia

INTRODUCTION

The West Sumatra region is highly susceptible to earthquakes due to its position near the convergent boundary between the Indo-Australian and Eurasian plates. In this zone, the Indo-Australian plate is subducting beneath the Eurasian plate, generating significant tectonic activity. The primary seismic sources in the region include the Megathrust zone, the Mentawai Fault, and the Sumatra Fault (Supendi *et al*., 2023).

On February 25, 2022, a magnitude 6.2 earthquake struck West Sumatra. The epicenter was located on land at a depth of approximately 10 km, about 17 km northeast of West Pasaman, on the slopes of Mount Talamau. This shallow crustal earthquake was attributed to active faulting along the Semangko Fault system, specifically on the previously unmapped Talamau Fault (Supendi *et al*., 2023).

Kajai Village, situated in the Talamau District of West Pasaman Regency and located near the earthquake's epicenter, suffered extensive destruction. Surface ruptures were observed in the area following the event. The earthquake likely altered the geological structure of local rock formations, increasing the susceptibility of the area to secondary hazards such as landslides and ground subsidence, especially due to the area's high sensitivity to seismic vibrations. These conditions contributed to widespread infrastructural damage, economic losses, and fatalities (Zulfiar *et al*., 2014).

To reduce the risk of loss of life and property, seismic vulnerability index mapping was conducted in Kajai Village. The seismic vulnerability index quantifies the susceptibility of the ground surface to damage and deformation during an earthquake. Higher index values indicate greater vulnerability. This index was derived from microtremor measurements, which were analyzed using the Horizontal-to-Vertical Spectral Ratio (HVSR) method. This technique calculates the dominant frequency and amplification factor

0126-6187; 2637-109X / Published by the Geological Society of Malaysia.
© 2026 by the Author(s). This is an open access article distributed under the terms of the Creative Commons Attribution (CC-BY) License 4.0.

of local soils by comparing the spectral amplitudes of the horizontal and vertical components of microtremor signals, as originally proposed by Nakamura (1989).

The primary objective of the seismic vulnerability index mapping in Kajai Village was to identify high-risk zones that are especially prone to earthquake-induced damage. These findings provide critical information for disaster risk reduction and are valuable for guiding development policies and spatial planning aimed at minimizing the impact of future seismic events (Fitri *et al*., 2018; Halimah & Octova, 2018; Ortega *et al*., 2019; Sapitri & Octova, 2021).

Earthquake

Earthquakes are vibrations or ground shaking that originate within the Earth and may result from various phenomena such as volcanic eruptions, landslides, bomb explosions, and other natural or artificial events. However, most earthquakes are caused by the movement of the Earth's crust along fault lines (Khan *et al*., 2019). According to the elastic rebound theory, earthquakes occur due to the sudden release of accumulated elastic strain energy in the lithosphere (Ibrahim & Subardjo, 2005).

The basic mechanism of an earthquake can be explained as follows: when two opposing forces act on rocks within the Earth's crust, the rocks undergo deformation due to their elastic properties (Arifudin, 2018). If this stress continues over time, the rock's strength will eventually be exceeded, leading to a sudden rupture along a fault plane. This process is illustrated in Figure 1. Once the stress surpasses the rock's threshold, the rock breaks and shifts abruptly along the fault, releasing the stored energy in the form of seismic waves. After the rupture, the rock returns to a new equilibrium state, but its shape or position may have changed. This rapid release of energy is what we perceive as an earthquake.

Microtremor

Microtremors are small, barely perceptible ground vibrations generated by human activities or natural atmospheric disturbances. In this context, ambient noise refers to continuous background seismic vibrations arising from various sources such as road traffic, industrial machinery, coastal wave action, and weather-related phenomena (Bukhori, 2011). This ambient noise primarily propagates through surface waves, notably Rayleigh waves (detectable via vertical seismic sensors) and Love waves (detectable via horizontal sensors).

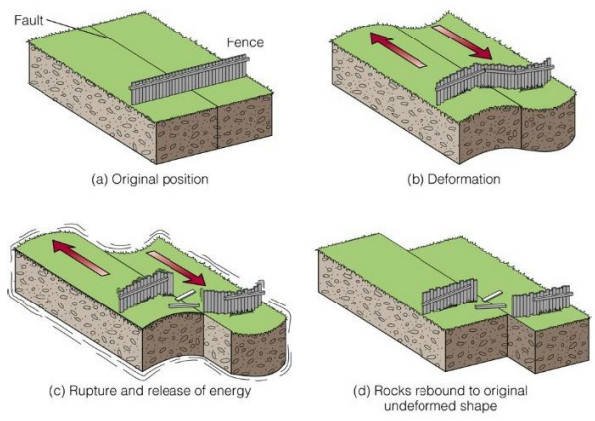


Figure 1: Earthquake mechanism (Monroe *et al*., 2006).

Microtremors can also be understood as natural harmonic vibrations of the soil that occur continuously, often trapped within surface sediment layers. These vibrations are reflected by the impedance contrast at subsurface boundaries and are typically generated by micro-scale ground motions and other environmental sources (Stanko *et al*., 2019). The characteristics of microtremors are closely linked to subsurface soil structures, making them useful for evaluating local geotechnical conditions. Through proper analysis, microtremor measurements can reveal the dynamic behavior of subsurface layers (Nakamura, 2000).

Microtremors are generally categorized by their dominant period: short-period microtremors (less than one second) typically indicate shallow subsurface structures with thicknesses of a few tens of meters, whereas long-period microtremors (greater than one second) suggest deeper soil layers (Molnar *et al*., 2018). In general, microtremors exhibit displacement amplitudes ranging from 0.1 to 1 μm and vibration velocities between 0.001 and 0.1 cm/s (Mirzaoglu & Dýkmen, 2003).

Microtremor analysis is widely conducted using the Horizontal-to-Vertical Spectral Ratio (HVSR) method, which has proven to be an effective technique for estimating site-specific seismic response characteristics from ambient vibration data. Originally introduced by Nogoshi and Igarashi in the 1970s, the HVSR method is based on the observed relationship between the horizontal-to-vertical spectral ratio of microtremors and the ellipticity of Rayleigh waves. This relationship forms the theoretical foundation for assessing site resonance characteristics (Nogoshi & Igarashi, 1971; Stanko *et al*., 2019). The method was later refined and popularized by Nakamura (1989) and has since gained global acceptance due to its non-invasive nature and efficiency in identifying site resonance conditions.

In practice, microtremor data are collected using a three-component seismometer that records ground motion along three axes: vertical (up-down), north–south, and east–west—corresponding to one vertical and two horizontal orthogonal components. The HVSR is calculated by taking the ratio of the average spectral amplitude of the horizontal components to that of the vertical component in the frequency domain. The resulting HVSR curve typically exhibits a prominent peak, which indicates the dominant frequency (f_0), representing the site's natural resonance frequency. The height of the peak corresponds to the amplification factor (A_0), reflecting the amplification potential of seismic waves due to contrasts in subsurface impedance (Nakamura, 2000; Ávila-Barrientos & Castro, 2016).

The amplification factor refers to the degree to which seismic ground motion is increased at the surface due to local soil conditions. It can be determined from the height of the peak in the HVSR spectrum obtained from microtremor data (Nakamura, 2000). To illustrate the HVSR analysis, Figure 2 presents a representative HVSR spectrum adapted from Octova *et al*. (2025). Each thin colored line represents the spectral ratio from an individual time window, while the thick black line denotes the average HVSR curve. The peak of the curve identifies the dominant frequency (f_0), and its amplitude represents the amplification factor (A_0). The gray-shaded band indicates the ±1 standard deviation range, providing insight into the statistical reliability of the recorded data. This type of spectral analysis is essential for evaluating site response and for calculating the seismic vulnerability index (K_g), especially in areas with complex subsurface conditions. Amplification factors are typically classified into four zones: low, medium, high, and very high. The classification adopted in this study follows Ratdomopurbo's criteria, as referenced in Haerudin *et al*. (2020), and is shown in Table 1.

Amplification occurs when seismic waves travel through subsurface layers with contrasting physical properties, such as transitions from stiff to soft soils. This phenomenon is primarily influenced by the impedance contrast between the surface and underlying layers, which is governed by the site's dynamic soil stiffness in multi-layered systems (Nakamura, 2005). A high impedance contrast results in a significant increase in wave amplitude, known as the amplification factor (A_0). This factor can be quantitatively determined from the peak height of the HVSR curve (Nakamura, 2000) and serves as a key indicator of a site's potential to amplify seismic ground motion.

The dominant frequency (f_0) represents the natural frequency of vibration associated with the local subsurface strata. It provides insights into the type and mechanical properties of the underlying soil. Local soil conditions significantly affect the behavior of seismic waves during an earthquake, making the dominant frequency a critical parameter in site characterization. Soil classification based on dominant frequency values, as proposed by Kanai, is presented in Table 2.

The seismic vulnerability index (K_g) quantifies the degree to which surface soil layers are susceptible to deformation during an earthquake (Arifudin, 2018). It reflects the combined influence of dominant frequency and amplification factor values, as well as surface-level measurements affected by seismic activity. These parameters can be used to estimate how vulnerable a region is to earthquake-induced ground motion.

Areas with high seismic vulnerability index values are typically characterized by low dominant frequency values.

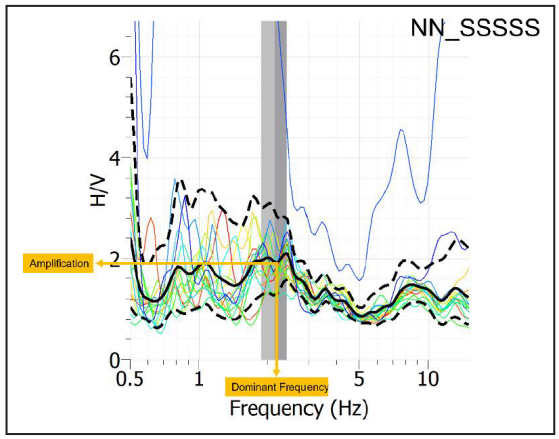


Figure 2: HVSR curve (Octova *et al*., 2025).

Table 1: Classification of amplification factor (Haerudin *et al*., 2020).

Classification	Amplification Factor Value
Low	< 3
Medium	3≤ < 6
High	6 ≤ < 9
Very High	≥ 9

Table 2: Soil classification based on dominant frequency value (Kanai, 1983).

Classification	Dominant Frequency	Soil Classification by Kanai	Soil Description
Type I	< 2.5	Alluvial rock formed from deltaic sedimentation, topsoil, silt, etc.	The thickness of the surface sediment is very thick
Type II	2.5-4	Alluvial rocks with a thickness of >5 m. It consists of sandy gravel, sandy hard clay, loam, etc.	The thickness of its surface sediment classified as thick category 10-30 m
Type III	4-6.6	Alluvial rocks with a thickness of 5 m. Consists of sandy-gravel, sandy hard clay, loam, etc.	The thickness of its surface sediment classified as middle category 5-10 m
Type IV	6.6-20	Tertiary rocks or older. It consists of Hard sandy rocks, gravels, etc.	Very thin sedimentary thickness dominated by hard rocks

This implies that regions with thick layers of soft sediments and low-frequency soils are more prone to severe earthquake damage. The seismic vulnerability index is defined under strain conditions at a scale of 10^{-6} s²/cm (Nakamura, 2000). The level of soil strain during seismic loading can be calculated using the following equation (Nakamura, 1997):

$$\gamma = \frac{A_g \delta}{H} \quad (1)$$

A_g is amplification factor, H is thickness of the soil layer, and δ is movement of seismic waves beneath the surface. Dominant amplification value (f_g) on the surface of the soil is formulated as:

$$f_g = \frac{v_s}{4H} \quad (2)$$

From this, the soil layer thickness can be formulated as:

$$H = \frac{v_s}{4f_g} \quad (3)$$

The dominant frequency at the subsurface can also be expressed as:

$$f_g = \frac{v_b}{4A_g H} \quad (4)$$

Nakamura (1997) also defines the bedrock acceleration as:

$$a_b = (2\pi f_g)^2 \delta \quad (5)$$

By substituting equations (4) and (5) into equation (1), we obtain:

$$\gamma = \frac{A_g a_b}{(2\pi f_g)^2} \frac{4A_g f_g}{v_b} = \frac{A_g^2}{f_g} \frac{a_b}{\pi^2 v_b} \quad (6)$$

If the efficiency of the dynamic force contributing to strain is e% of the static force, then the effective strain γ_e is:

$$\gamma_e = eK_g a_b \quad (7)$$

Thus, the seismic vulnerability index can be formulated as:

$$K_g = \frac{A_g^2}{f_g} \frac{1}{\pi^2 v_b} \quad (8)$$

Since v_b (bedrock shear wave velocity) tends to remain relatively constant within a region, the seismic vulnerability index effectively indicates local deformation potential at a given site. For simplicity, Nakamura (2008) proposed a more direct form for estimating the seismic vulnerability index:

$$K_g = \frac{A_0^2}{f_0} \quad (9)$$

K_g is seismic vulnerability index (× 10^{-6} s²/cm), A_0 is amplification factor, and f_0 is dominant frequency (Hz). A high K_g value indicates that the area is highly susceptible to seismic deformation and is commonly associated with soft sedimentary soils. Conversely, low K_g values suggest more stable ground conditions with stronger, more competent rock formations. Table 3 summarizes the K_g-based classification adopted in this study and serves as the bridge between the f_0–A_0 parameters and the mapped vulnerability zones.

Research area: Kajai Village, West Pasaman Regency

Kajai Village is located in the Talamau District of West Pasaman Regency, a region with a complex geological setting that plays a critical role in shaping its seismic behavior. According to the Lubuksikaping geological map (Rock *et al*., 1983), the area's stratigraphy includes a pre-Tertiary metamorphic basement and older sedimentary formations, overlain by extensive Quaternary volcanic deposits originating from Mount Talamau. The basement consists of metamorphic rocks from the Woyla Group, unconformably overlain by Tertiary sedimentary units such as the Silungkang and Kuantan Formations, which comprise limestone, sandstone, and shale, as well as Neogene volcanic rocks.

Mount Talamau, also referred to as Talakmau, is a Quaternary andesitic to dacitic composite volcano that has produced a range of deposits including lava flows, tuffs, and pyroclastic materials, which dominate the surrounding landscape (Suasti, 2024). Along with recent alluvial sediments, these volcanic products form the predominant lithology of West Pasaman, making the region largely volcanic in character. Igneous and sedimentary units are also exposed in several subregions. Figure 3 shows the geological map of Kajai Village, illustrating the spatial distribution of these formations within the study area.

In the vicinity of Kajai Village, the main surface units consist of Quaternary alluvium (Qh) and volcanic deposits from Mount Talamau (Qvta). The Qh unit comprises unconsolidated sand, gravel, and silt deposited by fluvial processes, while the Qvta unit represents products of Mount Talamau's eruptive history. Beneath these layers, older rocks

Table 3: Seismic vulnerability index value classification (Nakamura, 2008).

Classification	Seismic Vulnerability Index Value (K_g x 10-6 s²/cm)
Low	$K_g < 5$
Medium	$5 < K_g < 20$
High	> 20

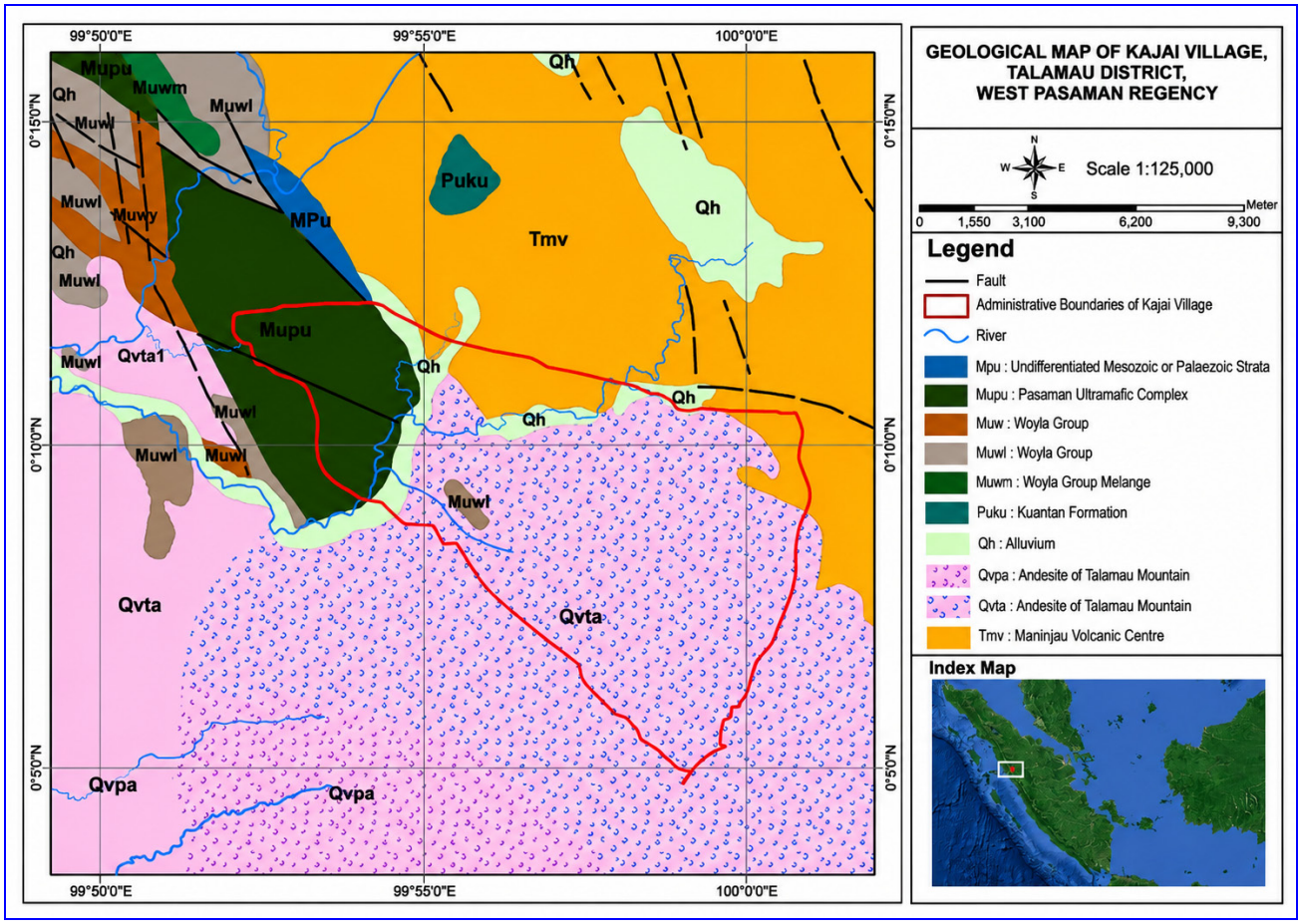


Figure 3: Geological map of Kajai Village (Rock *et al.*, 1983).

crop out in the surrounding terrain, including the Miocene-age Maninjau Volcanic Formation (Tmv), composed of andesitic lava and breccia, and the Pasaman Ultramafic Complex (Mupu), an intrusive unit. This geological sequence results in a highly heterogeneous subsurface profile, with soft, young surface deposits overlying more consolidated Tertiary volcanic and sedimentary rocks. The stratified crust reflects the geodynamic evolution of West Pasaman, shaped by both tectonic and volcanic activity.

Topographically, this stratigraphy is expressed in the form of river valleys and low-lying plains underlain by alluvial and volcanic fill, whereas older bedrock is exposed in higher elevations and along the slopes of Mount Talamau. Faulted and uplifted blocks contribute to steep terrain, which is highly susceptible to mass wasting. This vulnerability was evident during the 2022 earthquake, which triggered numerous slope failures in the region (Dewanto *et al*., 2022).

Tectonically, West Pasaman lies along the Great Sumatran Fault (GSF), a major strike-slip fault system extending across the island of Sumatra. The dominant structural feature in the study area is a local branch of the GSF known as the Talamau segment. Near Kajai, the GSF trends northwest–southeast and has historically been identified as a prominent lineament cutting through the Talamau range. While earlier interpretations considered this fault segment to be inactive, the shallow Mw 6.2 earthquake on February 25, 2022, confirmed its reactivation. This event was attributed to slip along the Talamau segment of the GSF (Supendi *et al*., 2023; Sinaga *et al*., 2023) and caused substantial damage to Kajai Village, which lies in close proximity to the fault trace. The presence of this active fault significantly increases the local seismic hazard, producing not only strong ground shaking but also surface deformation. Long-term tectonic deformation has fractured and weakened rocks along the fault zone, influencing soil development and enhancing the amplification of seismic waves (Iskarni *et al*., 2010; Suasti, 2024).

The lithological characteristics of the region play a central role in determining the behavior of seismic waves and, consequently, the level of seismic vulnerability. Generally, thick and unconsolidated Quaternary deposits tend to amplify seismic waves, while denser, more competent bedrock materials dampen ground motion. In Kajai Village, the subsurface consists of loose volcanic materials and alluvium such as pumice, volcanic ash, and pyroclastic soils, which are associated with low shear-wave velocities and function as natural amplifiers of seismic energy.

Another important geological factor affecting seismic risk is the potential for earthquake-induced ground failures,

particularly liquefaction and landslides. The presence of saturated, cohesionless sandy soils, especially in river valleys and alluvial plains, elevates the risk of liquefaction during strong shaking. This phenomenon occurs when water-saturated soils lose their shear strength and behave temporarily like a liquid. In Kajai Village, volcanic ash layers and unconsolidated alluvium increase this susceptibility (Fauziah & Yulfa, 2024). Additionally, the steep slopes of Mount Talamau, which are composed of weathered volcanic breccia and tuff, are highly prone to landslides when subjected to ground shaking. The combination of rugged topography and active faulting makes the region particularly vulnerable to earthquake-triggered landslides, as observed during the 2022 event (Dewanto *et al*., 2022).

The geological characteristics of Kajai Village are a critical determinant of its seismic vulnerability. The interaction between the active Talamau segment of the GSF and the region's variable lithology creates a high-risk seismic environment. Areas underlain by thick Quaternary deposits experience significant ground motion amplification, as reflected in elevated seismic vulnerability index (K_g) values, particularly in zones near the fault. This pattern is consistent with HVSR analysis results, which identify low-frequency and high-amplification sites as the most susceptible to seismic damage. In contrast, areas with shallow bedrock and more competent substrates show lower amplification and reduced seismic vulnerability. This geological context provides essential insight for interpreting HVSR data and assessing seismic risk. It highlights why certain areas are more prone to damage during seismic events. Ultimately, Kajai's geological profile, characterized by a Quaternary volcanic setting intersected by an active strike-slip fault, requires that seismic hazard assessments account for both earthquake source characteristics and local site amplification effects. Recent studies (Sinaga *et al*., 2023; Suasti, 2024; Fauziah & Yulfa, 2024) emphasize the need for mitigation strategies tailored to the unique geological conditions of the Talamau District.

METHODOLOGY

Microtremor analysis in this study was conducted using the Horizontal-to-Vertical Spectral Ratio (HVSR) method, a widely adopted technique for estimating seismic site characteristics through non-invasive surface measurements. This approach enables the identification of key parameters such as dominant frequency (f_0), amplification factor (A_0), and seismic vulnerability index (K_g), which are critical for evaluating local site response.

Data acquisition

Microtremor data were collected in September 2022 during a field campaign in Kajai Village aimed at characterizing local seismic site conditions. The acquisition system consisted of an SL06 seismograph recorder (Figure 4a) and a Lennartz LE-3D/5s sensor (Figure 4b), forming a portable three-component seismometer setup. The Lennartz sensor is designed to detect low-frequency ambient vibrations with a corner frequency of 0.2 Hz, making it well suited for HVSR analysis due to its sensitivity to Rayleigh waves. The SL06 recorder functions as a high-resolution digital logger with time synchronization capability, ensuring accurate signal capture.

Microtremor measurements were conducted at 15 locations across Kajai Village, with each sensor recording ground motion in three directions: vertical, North–South, and East–West (Figure 4c). Each measurement lasted approximately 45 minutes at a sampling rate of 100 Hz. Fieldwork was carried out under stable weather conditions to minimize anthropogenic and environmental noise. Measurement sites were selected based on surface morphology

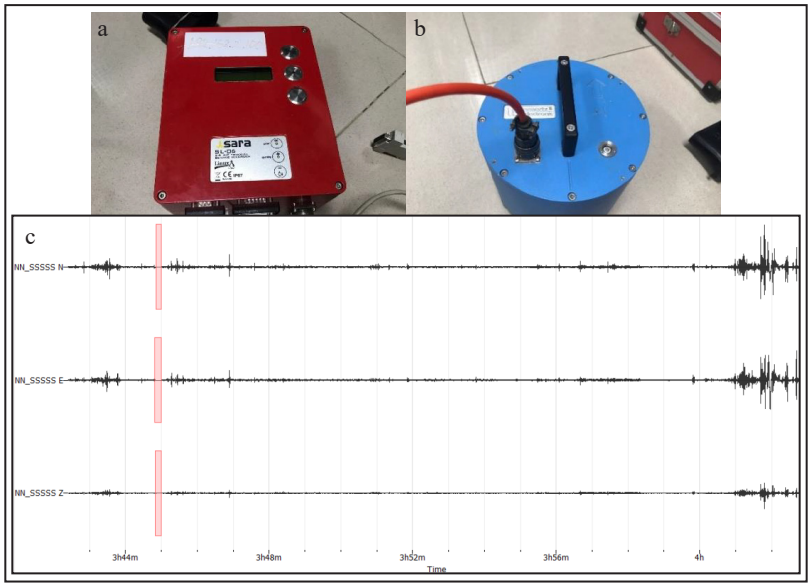


Figure 4: a. Recorder SL06 Seismograph; b. Sensor Lennartz LE-3D/5s; c. Three-component vibration data showing vertical, North–South, and East–West components.

and their proximity to geological structures such as fault zones, slopes, and sedimentary boundaries. This site selection ensured the spatial representativeness and quality of the recorded ambient noise data for subsequent HVSR analysis.

Data processing and spectral analysis

Time-series data were processed using GEOPSY software. Time windows of 30–40 seconds were selected to isolate stationary microtremor segments, excluding transient signals caused by human activity or environmental disturbances (Figure 5). A Fast Fourier Transform (FFT) was applied to convert the time-domain signals into the frequency domain. The HVSR curve was generated by computing the geometric mean of the two horizontal components (North–South and East–West) and dividing it by the vertical component. The resulting HVSR spectrum characterizes the frequency-dependent amplification behavior of the subsurface.

Determination of seismic parameters

The dominant frequency (f_0) is defined as the frequency at which the HVSR curve reaches its maximum peak. The amplification factor (A_0) is the corresponding amplitude value at this peak. These values were extracted from each HVSR curve and used to evaluate local site response. Representative f_0 and A_0 values from all measurement points were used to assess spatial variations in site conditions across Kajai Village. While specific results are detailed in the subsequent section, this methodology consistently identifies the HVSR peak as an indicator of both amplification potential and resonance characteristics. Soil classification and seismic vulnerability assessments were conducted based on the distribution and range of f_0 and A_0 values observed across the study area.

RESULTS

Following the processing of microtremor data, the HVSR method was applied to generate frequency response curves. As shown in Figure 6, the peak of each HVSR curve represents the dominant frequency (f_0), while the corresponding amplitude indicates the amplification factor (A_0). These parameters describe how seismic waves interact with subsurface materials and form the basis for evaluating seismic vulnerability across Kajai Village.

Dominant frequency (f_0) values observed in the study area range from 0.66 Hz to 12.58 Hz. According to the Kanai soil classification system, these frequencies correspond to different subsurface conditions, ranging from soft alluvium to shallow bedrock. The classification of soil types based on f_0 includes: Type I ($f_0 < 2.5$ Hz), Type II (2.5 Hz $\leq f_0 < 4$ Hz), Type III (4 Hz $\leq f_0 < 6.6$ Hz), and Type IV ($f_0 \geq 6.6$ Hz).

Table 4 provides the complete dataset of f_0, A_0, and seismic vulnerability index (K_g) values at each measurement point.

- Type I soils, found at Points 1, 2, 3, 5, 7, 8, 9, 10, and 13, are characterized by low dominant frequencies ($f_0 < 2.5$ Hz), indicating thick, unconsolidated sediments. These locations are more prone to wave trapping and amplification, typically resulting in higher seismic vulnerability.
- Type II soils, observed at Points 4 and 15, have f_0 values between 2.5 Hz and 4.0 Hz, reflecting moderately thick sediment layers. These areas experience moderate seismic amplification.

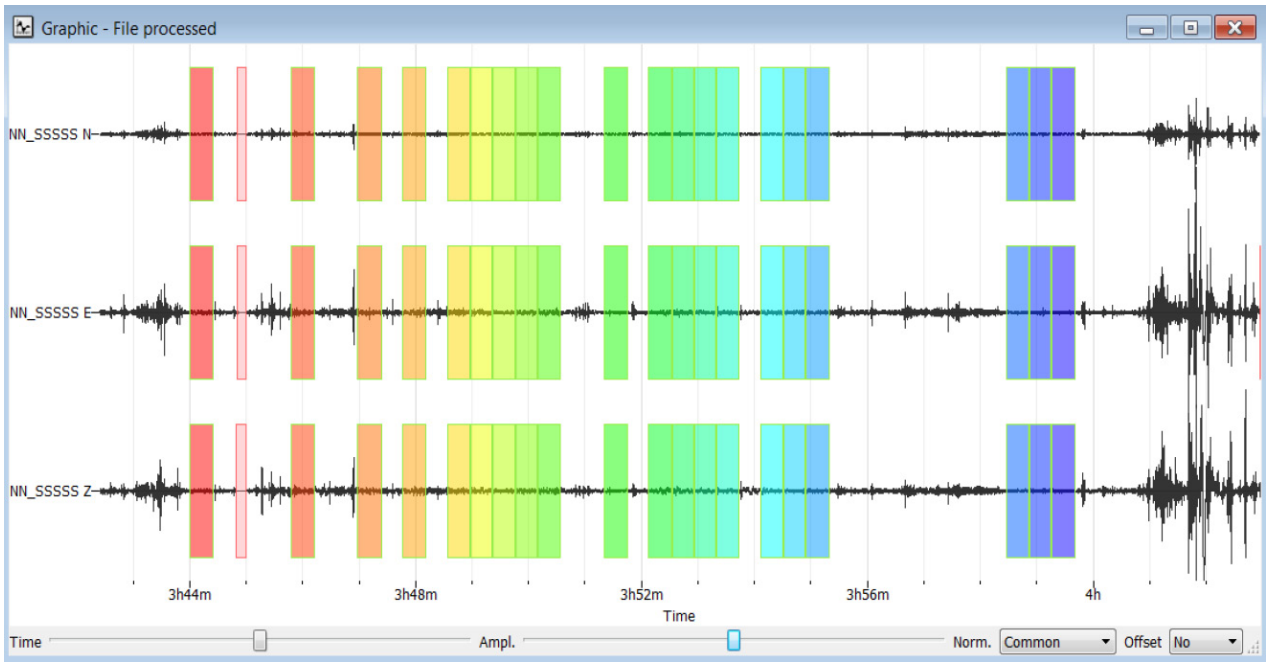


Figure 5: Selected time windows for HVSR analysis.

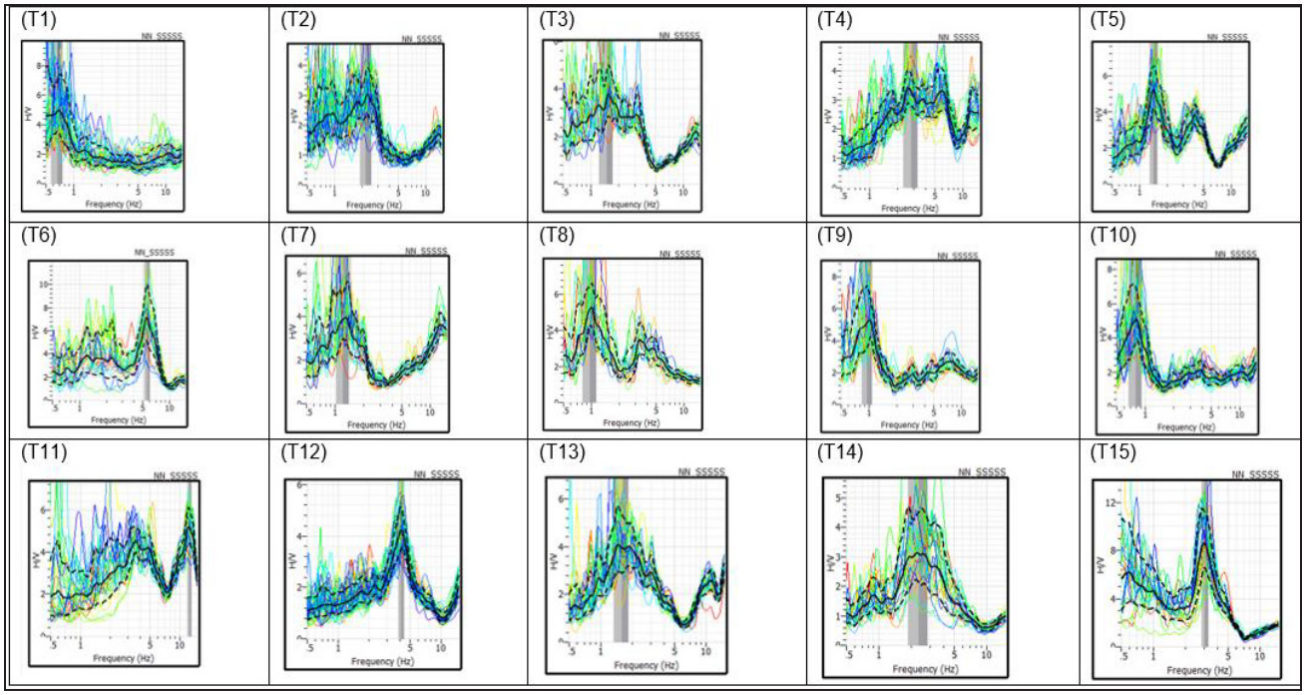


Figure 6: HVSR curve at measurement point.

Table 4: Seismic data results of dominant frequency, amplification factor, and seismic vulnerability index.

Point	Latitude	Longitude	f_0 (Hz)	Soil Classification According to Kanai	A_0	Amplification Classification	Seismic Vulnerability Index (x 10^{-6} s^2/cm)	Vulnerability Classification
1	00008’31.3’’N	099059’43.1’’E	0.66	Type I	4.86	Medium	35.79	High
2	00009’25.6’’N	099059’59.6’’E	2.22	Type I	2.95	Low	3.92	Low
3	00009’33.2’’N	099058’42.4’’E	1.48	Type I	3.53	Medium	8.42	Medium
4	00010’24.1’’N	099058’41.8’’E	2.81	Type II	3.28	Medium	3.83	Low
5	00010’45.0’’N	099057’52.8’’E	1.43	Type I	5.19	Medium	18.84	Medium
6	00010’18.1’’N	099056’45.5’’E	5.67	Type III	7.03	High	8.72	Medium
7	00010’00.9’’N	099056’14.9’’E	1.22	Type I	3.86	Medium	12.21	Medium
8	00009’40’’N	099055’39.2’’E	0.97	Type I	5.18	Medium	27.66	High
9	00009’29.4’’N	099055’49.7’’E	0.95	Type I	5.07	Medium	27.06	High
10	00009’10.1’’N	099056’15.7’’E	0.79	Type I	5.03	Medium	32.03	High
11	00008’59.1’’N	099055’36.3’’E	12.58	Type IV	5.15	Medium	2.11	Low
12	00010’03.2’’N	099055’03.2’’E	4.15	Type III	4.21	Medium	4.27	Low
13	00010’27’’N	099055’27.6’’E	1.58	Type I	3.95	Medium	9.88	Medium
14	00010’56.7’’N	099054’54.9’’E	2.36	Type I	3.09	Medium	4.05	Low
15	00011’46.7’’N	099054’24.7’’E	3.06	Type II	8.5	High	23.61	High

- Type III soils, at Points 6 and 12, show f_0 values from 4.0 Hz to 6.6 Hz, indicating thinner sediment layers or partially weathered rock with generally lower amplification potential.
- Type IV soils, represented by Point 11 ($f_0 \geq 6.6$ Hz), are associated with shallow or exposed bedrock and show low susceptibility to amplification.

The spatial distribution of dominant frequency across Kajai Village is illustrated in Figure 7, highlighting low-frequency zones concentrated in the central and southern regions, where thick soft sediments are dominant. These areas are more likely to amplify seismic waves during an earthquake (Susilanto *et al*., 2016).

Amplification factor (A_0) values across the study area range from 2.95 to 8.50, reflecting varying subsurface impedance contrasts.

- Most points, including 1, 3, 5, 7, 8, 9, 10, and 13, exhibit medium amplification ($3 \leq A_0 < 6$), indicating moderate seismic risk, particularly when coupled with low f_0 values.
- High amplification values ($A_0 \geq 6$) were recorded at Points 6 and 15, suggesting elevated potential for ground motion intensification.
- Low amplification ($A_0 < 3$) was observed at Point 2, corresponding with higher f_0 and lower seismic vulnerability.

Regions with high amplification factors are more likely to experience severe damage during seismic events due to the increased energy of the seismic waves as they travel through softer sediments (Arifudin, 2018). Figure 8 shows the spatial distribution of amplification factors, which aligns with variations in geological structure and topography across the study area.

The seismic vulnerability index (K_g), calculated using the formula $K_g = A_0^2 / f_0$, quantifies a site's susceptibility to seismic damage. Based on this index, each point in Kajai Village was classified into low, medium, or high vulnerability zones. The spatial variation of K_g values is presented in Figure 9, while detailed numerical data for each point is provided in Table 4.

High vulnerability ($K_g > 20 \times 10^{-6}$ s²/cm) was identified at Points 1, 8, 9, 10, and 15. These areas share the characteristics of low dominant frequency and moderate-to-high amplification, often corresponding to soft and thick sedimentary deposits.

Moderate vulnerability ($5 < K_g \leq 20 \times 10^{-6}$ s²/cm) was observed at Points 3, 5, 6, 7, and 13, indicating intermediate site conditions.

Low vulnerability ($K_g < 5 \times 10^{-6}$ s²/cm) was recorded at Points 2, 4, 11, 12, and 14, where stiffer subsurface materials or bedrock dominate.

Point 11, for example, lies over hard bedrock and is geologically stable, placing it in the low-risk category (Nubatonis *et al*., 2017).

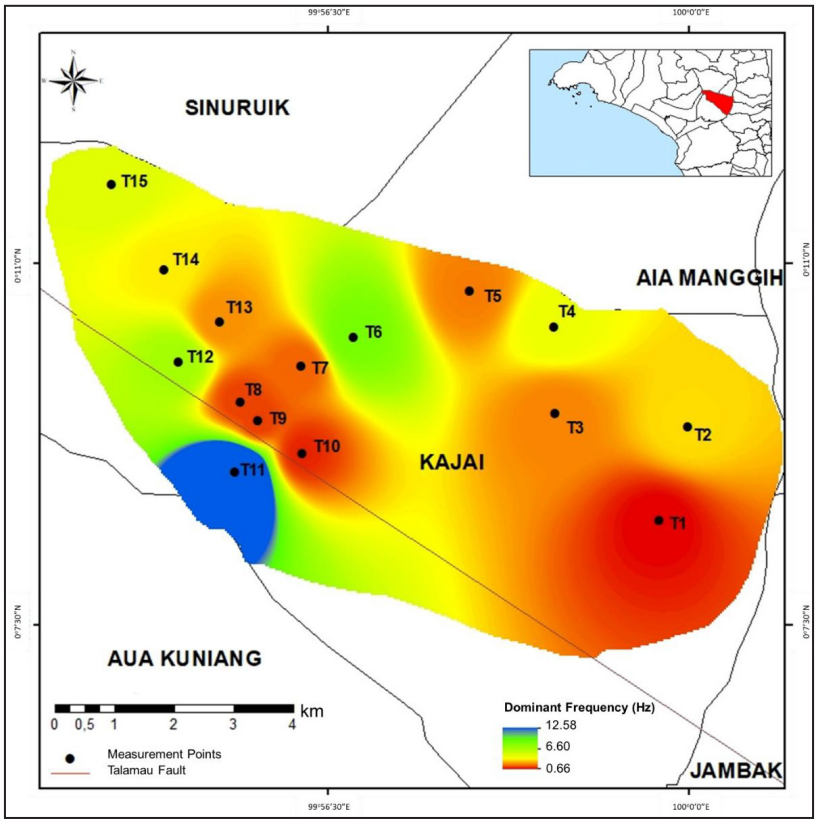


Figure 7: Dominant Frequency Map.

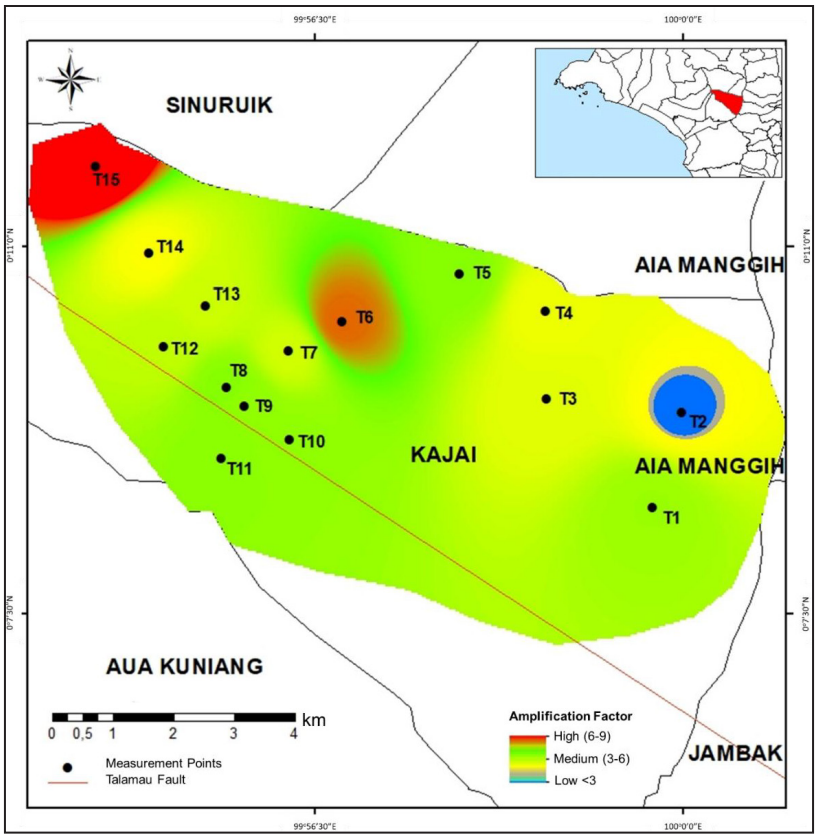


Figure 8: Amplification Factor Map.

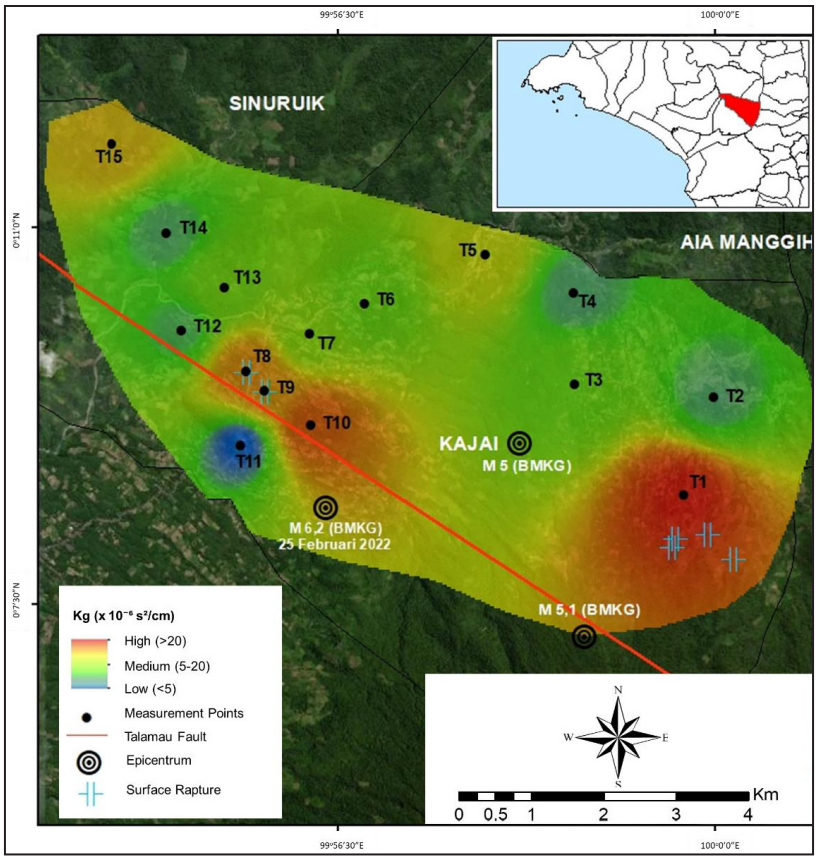


Figure 9: Seismic Vulnerability Index Map. Background basemap is from Google Earth.

The seismic vulnerability index model in Figure 10 reveals a clear correlation between high K_g values and proximity to the Talamau Fault. Points 1, 8, and 9, which show the highest K_g values, are located near this fault, demonstrating the significant impact of active tectonic structures on surface vulnerability (Supendi *et al*., 2023).

These findings indicate that sites with low f_0 and moderate-to-high A_0 are associated with elevated seismic vulnerability (K_g). The spatial distribution of these indices emphasizes the need for location-specific mitigation strategies, especially in areas near fault zones such as the Talamau segment. These results serve as the foundation for the risk assessment discussed in the following section.

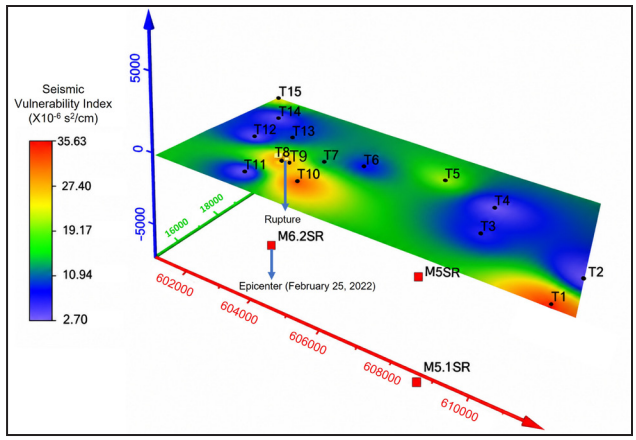


Figure 10: Seismic Vulnerability Index Modeling.

DISCUSSION

The results of this study reveal significant spatial variability in seismic response across Kajai Village, primarily driven by variations in dominant frequency (f_0), amplification factor (A_0), and the resulting seismic vulnerability index (K_g). These parameters, derived from microtremor HVSR analysis, offer detailed insights into subsurface conditions and their influence on ground motion during seismic events.

Areas characterized by low dominant frequencies (< 2.5 Hz), particularly in the central and southern parts of the village, indicate the presence of thick, unconsolidated sediments. These zones strongly correlate with elevated amplification factors and high K_g values, indicating an increased risk of seismic wave trapping and ground motion amplification. Such conditions are typical of alluvial environments, where energy from seismic waves is retained and intensified due to impedance contrasts between soft surface sediments and underlying bedrock (Susilanto *et al*., 2016). In contrast, zones with high dominant frequencies (≥ 6.6 Hz), such as those near Point 11, suggest shallow bedrock or thin, stiff sedimentary layers. These conditions result in lower amplification and minimal resonance, reflecting more stable subsurface conditions with reduced seismic vulnerability (Nubatonis *et al*., 2017).

The amplification factor (A_0) plays a crucial role in differentiating risk levels. Moderate amplification ($3 \leq A_0 < 6$) is widespread across the village and contributes to medium seismic vulnerability in areas with moderate sediment thickness. However, amplification values exceeding 6, as observed at Points 6 and 15, significantly elevate K_g values, particularly when coupled with low f_0 values. This interplay highlights the nonlinear relationship between f_0 and A_0, where even moderate amplification in low-frequency zones can result in severe ground shaking potential (Nakamura, 2008; Arifudin, 2018).

The spatial model of the seismic vulnerability index (Figure 9) clearly illustrates these dynamics. Points with the highest K_g values are primarily located near active structural features, especially the Talamau Fault. This suggests that proximity to fault zones increases both geological complexity and seismic hazard. These findings are consistent with previous studies that emphasize the combined effects of surface sedimentation, fault proximity, and ground motion amplification (Supendi *et al*., 2023).

The HVSR method has proven to be a valuable tool for seismic microzonation and risk mitigation, especially in data-scarce or rural areas. In such contexts, traditional seismic methods such as borehole drilling are often impractical due to financial and logistical constraints. Using f_0 and A_0 values derived from microtremor measurements provides a cost-effective and non-invasive alternative for identifying seismic hazards. Past studies in locations like Palu and Bengkulu have demonstrated that HVSR can effectively detect subsurface resonance phenomena associated with sediment thickness, thereby guiding more localized seismic zoning (Salsabila *et al*., 2023; Siburian *et al*., 2024).

Moreover, integrating HVSR data with other geophysical methods, such as seismic refraction or MASW, enhances the resolution of subsurface imaging. This combined approach improves estimates of bedrock depth, particularly in sediment-filled basins or geologically complex settings (Rahmania *et al*., 2023; Maniscalco & Ebel, 2025). Such integration offers strategic advantages in regions where direct geological data are limited or unavailable.

Compared to traditional subsurface investigation techniques, HVSR is significantly more accessible and requires minimal instrumentation. It allows for rapid site assessments over large areas and provides robust data on local site effects, which are critical for designing earthquake-resilient infrastructure (Zhang *et al*., 2021; Ryanto *et al*., 2022). This is especially relevant in Kajai Village, where limited resources necessitate efficient and scalable hazard-mapping solutions.

The significance of the K_g index extends beyond quantifying seismic vulnerability. It also plays a critical role in informing policy. Vulnerability mapping using Kg values has influenced revisions to building codes and the development of disaster mitigation frameworks in several tectonically active regions (Parsizadeh *et al*., 2015). In

areas like West Sumatra, the findings of this study highlight the urgent need for stricter zoning regulations and the incorporation of seismic vulnerability data into infrastructure planning (Zulfiar *et al.*, 2014).

Seismic assessments based on HVSR also inform land-use policy by identifying zones that require priority for reinforcement or retrofitting. This information is especially essential for urban planners in regions with limited resources, as it enables the efficient allocation of disaster mitigation efforts (Susilo *et al*., 2024). Increasingly, community-based disaster risk reduction (DRR) strategies are incorporating HVSR microzonation into localized planning. For example, in Bengkulu, HVSR data have been used to develop seismic hazard maps that guide construction practices and community resilience programs (Siburian *et al*., 2024). The integration of such data with social vulnerability indices using GIS platforms has further enhanced public awareness and strengthened community engagement in disaster preparedness (Sauti *et al*., 2020; Molua *et al*., 2024).

Overall, this study underscores the value of HVSR-based microtremor assessments in identifying site-specific seismic risks. The integration of f_0, A_0, and K_g offers a multidimensional perspective of seismic vulnerability that is critical for guiding local disaster mitigation, zoning regulation, and engineering design. It reinforces the need for tailored risk reduction strategies in areas with thick sedimentary cover and active fault lines.

This research contributes meaningfully to seismic microzonation efforts in data-limited settings such as Kajai Village, demonstrating the effectiveness of HVSR analysis in identifying localized seismic vulnerabilities. The findings offer a scientific foundation for future land-use planning, infrastructure development, and community-based DRR programs in West Sumatra and similar seismically active regions.

In particular, the study's findings emphasize the need for targeted mitigation strategies in high-vulnerability zones where low dominant frequencies and high amplification factors converge. Building codes in these areas should be updated to require structural reinforcement to reduce potential damage during earthquakes. Additionally, the development of community preparedness programs and the implementation of early warning systems are critical to reducing overall risk to life and property (Gaudio *et al*., 2008; Ortega *et al*., 2019).

CONCLUSION

This study employed the Horizontal-to-Vertical Spectral Ratio (HVSR) method to evaluate site-specific seismic vulnerability in Kajai Village, West Pasaman Regency, an area that was severely affected by the 2022 Mw 6.2 earthquake. Microtremor data collected from 15 measurement points were used to derive dominant frequency (f_0), amplification factor (A_0), and seismic vulnerability index (K_g), which revealed considerable spatial variation in seismic response throughout the study area. Zones with low f_0 values combined with moderate to high A_0 values, particularly those underlain by thick and unconsolidated sediments, showed high levels of seismic vulnerability. These zones were especially concentrated near the Talamau Fault, where the presence of active tectonic structures further intensified seismic risk. In contrast, locations with high f_0 and low A_0 values, typically associated with shallow bedrock, were found to have lower vulnerability levels. The findings confirm that the HVSR method is an effective, non-invasive, and cost-efficient tool for seismic microzonation, particularly in rural areas or regions with limited geological data. Moreover, the K_g index proved to be a reliable metric for translating site effect parameters into actionable indicators of seismic risk. This research advances the understanding of how geological and tectonic settings influence seismic vulnerability and provides essential information for improving regional earthquake resilience. The results underscore the importance of implementing targeted mitigation strategies, including the reinforcement of local building codes, prioritization of retrofitting efforts, and integration of seismic risk assessments into spatial and infrastructure planning. In addition, enhancing community preparedness and establishing early warning systems are critical actions for minimizing the human and economic impacts of future earthquakes. The methodology and outcomes of this study can serve as a model for other earthquake-prone regions with similar geological conditions, both in Indonesia and internationally, supporting the development of site-specific disaster risk reduction strategies.

ACKNOWLEDGEMENT

The author would like to thank Lembaga Penelitian dan Pengabdian Masyarakat Universitas Negeri Padang for funding this work. The authors also express gratitude to all parties involved. We would also like to express our sincere gratitude to the reviewers who have reviewed and evaluated this article. The comments and suggestions provided to improve this article are highly appreciated.

AUTHORS CONTRIBUTION

AO: Conceptualization, methodology, supervision. MIKAA: Review and editing. HAR: investigation, data collection. DY: Data collection. AHB: Data collection, formal analysis and project administration. YMA: Investigation, fieldwork coordination and project administration. RM: Investigation, and resources. MG: Investigation. SS: Visualization, investigation, data collection.

CONFLICT OF INTEREST

The authors declare that this research is free from conflicts of interest and that there are no personal relationships that could potentially influence the results presented in this paper.

REFERENCES

Arifudin, A.M., 2018. Site characteristics and seismic vulnerability in Klaten Regency using the Horizontal-to-Vertical Spectral Ratio (HVSR) method from microtremor data. Master's thesis, Universitas Islam Indonesia. (in Indonesian)

Ávila-Barrientos, L. & Castro, R.R., 2016. Site response of the Nars-baja and Resban broadband networks of the Gulf of California, México. Geofisica Internacional, 55(2). https://doi.org/10.22201/igeof.00167169p.2016.55.2.1717.

Bukhori, I.A., 2011. Mapping disaster-prone areas based on microseismic data using TDS (TIME Digital Seismograph) Type 303 S. Neutrino, 3(2), 154869. (in Indonesian)

Dewanto, B.G., Priadi, R., Heliani, L.S., Natul, A.S., Yanis, M., Suhendro, I., & Julius, A.M., 2022. The 2022 Mw 6.1 Pasaman Barat, Indonesia Earthquake, Confirmed the Existence of the Talamau Segment Fault Based on Teleseismic and Satellite Gravity Data. Quaternary, 5(4), 45. https://doi.org/10.3390/quat5040045.

Fauziah, N. & Yulfa, A., 2024. Microzonation mapping of building damage after earthquake disaster in Nagari Kajai West Pasaman District. Eighth Geoinformation Science Symposium 2023: Geoinformation Science for Sustainable Planet. https://doi.org/10.1117/12.3009712.

Fitri, D.A., Octova, A., & Anaperta, Y.M., 2018. Seismic vulnerability index zoning mapping in the post-mining area at PT Bukit Asam (Persero) Tbk., Ombilin Mining Unit, Sawahlunto. Bina Tambang, 3(2), 756–779. (in Indonesian)

Gaudio, V.D., Coccia, S., Wasowski, J., Gallipoli, M.R., & Mucciarelli, M., 2008. Detection of directivity in seismic site response from microtremor spectral analysis. Natural Hazards and Earth System Sciences, 8(4), 751–762. https://doi.org/10.5194/nhess-8-751-2008.

Haerudin, N., Rustadi, Alami, F., & Yogi, I.B.S., 2020. The effect site analysis based on microtremor data using the Horizontal to Vertical Spectral Ratio (HVSR) method in the Bandar Lampung City. Journal of Physics: Conference Series, 1572(1), 012075. https://doi.org/10.1088/1742-6596/1572/1/012075.

Halimah, H., & Octova, A., 2018. Ground vibration analysis for designing a stable slope in limestone mining, CV Tekad Jaya Halaban, 50 Kota Regency, West Sumatra. Bina Tambang, 3(4), 1784–1792. (in Indonesian)

Ibrahim, G. & Subardjo, 2005. Seismology Knowledge. Badan Meteorologi dan Geofisika, Jakarta. 108 p. ISBN 979-99507-0-8. (in Indonesian)

Iskarni, P., Antomi, Y., Yulfa, A., Purwaningsih, E. & Triyatno, 2010. Final Report on Visualization of the Potential of West Pasaman Regency in Multimedia Format. Pemerintah Kabupaten Pasaman Barat, Badan Perencanaan Pembangunan Daerah bekerja sama dengan Pusat Pengembangan Infrastruktur Data Spasial (PPIDS), Universitas Negeri Padang, Padang. 48 p. (in Indonesian)

Kanai, K., 1983. Engineering Seismology. University of Tokyo Press, Tokyo. 251 p.

Khan, K.A., Zaman, K., Shoukry, A.M., Sharkawy, A., Gani, S., Sasmoko, Ahmad, J., Khan, A., & Hishan, S.S., 2019. Natural disasters and economic losses: Controlling external migration, energy and environmental resources, water demand, and financial development for global prosperity. Environmental Science and Pollution Research, 26(14), 14287–14299. https://doi.org/10.1007/s11356-019-04755-5.

Maniscalco, S. & Ebel, J., 2025. Geophysical imaging of the subsurface seismic structure of the Chestnut Hill reservoir earth embankment dam (Massachusetts). Near Surface Geophysics, 23(2), 105-120. https://doi.org/10.1002/nsg.12330.

Mirzaoglu, M., & Dýkmen, Ü., 2003. Application of microtremors to seismic microzoning procedure. Journal of the Balkan Geophysical Society, 6(3), 143-156.

Molnar, S., Cassidy, J.F., Castellaro, S., Cornou, C., Crow, H., Hunter, J.A., Matsushima, S., Sánchez-Sesma, F.J., & Yong, A., 2018. Application of Microtremor Horizontal-to-Vertical Spectral Ratio (MHVSR) Analysis for Site Characterization: State of the Art. Surveys in Geophysics, 39(4), 613–631. https://doi.org/10.1007/s10712-018-9464-4.

Molua, C.O., Vwavware, J.O., & Chukwunwike, O., 2024. Seismic hazard assessments for Nigeria's urban centers. Earth Sciences Pakistan, 8(1), 19-27. https://doi.org/10.26480/esp.01.2024.19.27.

Monroe, J., Reed, W., & Richard, W. H.,2006. Physical Geology Exploring the Earth, 6th Edition. Brooks/Cole-Thompson, U.S.A. 690 p. ISBN-13: 978-0495011484.

Nakamura, N., 2005. A practical method for estimating dynamic soil stiffness on surface of multi-layered soil. Earthquake Engineering & Structural Dynamics, 34(11), 1391–1406. https://doi.org/10.1002/eqe.487.

Nakamura, Y., 1989. A method for dynamic characteristics estimation of subsurface using microtremor on the ground surface. Quarterly Report of Railway Technical Research, 30, 25-33.

Nakamura, Y., 1997. Seismic vulnerability indices for ground and structures using microtremor. In World Congress on Railway Research, Florence, Italy.

Nakamura, Y., 2000. Clear identification of fundamental idea of Nakamura's technique and its applications. In Proceedings of the 12th World Conference on Earthquake Engineering (Vol. 2656, pp. 1-8). Auckland, New Zealand.

Nakamura, Y., 2008. On The H/V spectrum. In 14th World Conference on Earthquake Engineering. Beijing, China, October 12-17, 2008.

Nogoshi, M. & Igarashi, T., 1971. On the Amplitude Characteristics of Microtremor. Journal of the Seismological Society of Japan (Zisin), 24(1), 26–40 (in Japanese with an English abstract). https://doi.org/10.4294/zisin1948.24.1_26.

Nubatonis, I., Sianturi, H.L., & Bernandus, B., 2017. Seismic microzonation mapping in Lili Village, Fatuleu District, Kupang Regency. Jurnal Fisika: Fisika Sains dan Aplikasinya, 2(2), 50–57. (in Indonesian)

Octova, A., Hashim, M.H.M., Simatupang, T.S., Febriandika, H., Gusman, M., & Yulhendra, D., 2025. Integrated passive seismic and geoelectrical resistivity methods for cavity identification in limestone quarry. Journal of Applied Geophysics, 241, 105836. https://doi.org/10.1016/j.jappgeo.2025.105836.

Ortega, J., Vasconcelos, G., Rodrigues, H., & Correia, M., 2019. A vulnerability index formulation for the seismic vulnerability assessment of vernacular architecture. Engineering Structures, 197, 109381. https://doi.org/10.1016/j.engstruct.2019.109381.

Parsizadeh, F., Ibrion, M., Mokhtari, M., Lein, H., & Nadim, F., 2015. Bam 2003 earthquake disaster: on the earthquake risk perception, resilience and earthquake culture – cultural beliefs and cultural landscape of Qanats, gardens of Khorma trees and Argh-e Bam. International Journal of Disaster Risk Reduction, 14, 457-469. https://doi.org/10.1016/j.ijdrr.2015.09.011.

Rahmania, R., Rasmid, R., Arisalwadi, M., & Sastrawan, F., 2023. Microzonation mapping in supporting construction

plan, new capital city of Indonesia (Case study: Sepaku Sub-district, Panajam Paser Utara Regency). Proceedings of the 4th International Seminar on Science and Technology (ISST 2022). https://doi.org/10.2991/978-94-6463-228-6_10.

Rock, N.M.S., Aldiss, D.T., Aspden, J.A., Clarke, M.C.G., Djunuddin, A., Kartawa, W., Miswar, Thompson, S.J. & Whandoyo, R., 1983. Geologic Map of the Lubuksikaping Quadrangle, Sumatra. Scale 1:250 000. Puslitbang Geologi Bandung.

Ryanto, T., Iswanto, E., Suryanto, S., Suntoko, H., Yuliastuti, Y., & Susiati, H., 2022. Site characterization study with microtremor data: A case study at the West Borneo npp potential site. Near Surface Geophysics, 20(5), 531-543. https://doi.org/10.1002/nsg.12233.

Salsabila, R., Yudistira, T., & Tohari, A., 2023. Mapping of soil dynamic response of palu city based on horizontal to vertical spectral ratio (HVSR) method. IOP Conference Series Earth and Environmental Science, 1288(1), 012019. https://doi.org/10.1088/1755-1315/1288/1/012019.

Sapitri, L.A. & Octova, A., 2021. Seismic vulnerability index zoning mapping in the mining area of CV Bara Mitra Kencana, Talawi District, Sawahlunto. Jurnal Bina Tambang, 6(5), 195–201. (in Indonesian). https://doi.org/10.24036/bt.v6i5.115182.

Sauti, N.S., Daud, M.E., & Kaamin, M., 2020. Construction of an Integrated Social Vulnerability Index to Identify Spatial Variability of Exposure to Seismic Hazard in Pahang, Malaysia. International Journal of Design & Nature and Ecodynamics, 15(3), 365–372. https://doi.org/10.18280/ijdne.150310.

Siburian, B., Marzuki, M., & Lubis, A., 2024. Local site effects and seismic microzonation around Suban area, Curup Rejang Lebong, Bengkulu deduced by ambient noise measurements. Geoenvironmental Disasters, 11(1), article 5. https://doi.org/10.1186/s40677-024-00268-7.

Sinaga, V.I.C., Aolindar, M.A.F., Pramudita, M.A.N., Supendi, P., Kirana, K.H., & Hasanah, M.U., 2023. Relocation of earthquake hypocenter using double-difference method in western part of sumatera. Journal of Physics: Conference Series, 2582(1), 012004. https://doi.org/10.1088/1742-6596/2582/1/012004.

Stanko, D., Markušić, S., Gazdek, M., Sanković, V., Slukan, I., & Ivančić, I., 2019. Assessment of the seismic site amplification in the city of Ivanec (NW part of Croatia) using the microtremor HVSR method and equivalent-linear site response analysis. Geosciences, 9(7), 312. https://doi.org/10.3390/geosciences9070312.

Suasti, Y., 2024. Development of active fault mapping method using geoelectric and geographical information system. International Journal of GEOMATE, 26(116), 72-84. https://doi.org/10.21660/2024.116.4360.

Supendi, P., Rawlinson, N., Prayitno, B.S., Sianipar, D., Simanjuntak, A., Widiyantoro, S., Palgunadi, K.H., Kurniawan, A., Shiddiqi, H.A., Nugraha, A.D., Sahara, D.P., Daryono, D., Triyono, R., Adi, S.P., Karnawati, D., Daniarsyad, G., Ahadi, S., Fatchurochman, I., Anugrah, S.D., Heryandoko, N., & Sudrajat, A., 2023. A previously unidentified fault revealed by the February 25, 2022 (Mw 6.1) Pasaman Earthquake, West Sumatra, Indonesia. Physics of the Earth and Planetary Interiors, 334, 106973. https://doi.org/10.1016/j.pepi.2022.106973.

Susilanto, P., Ngadmanto, D., Daryono, D., Hardy, T., & Pakpahan, S., 2016. Application of the HVSR microtremor method for determining seismic dynamic response in Padang City. Jurnal Lingkungan dan Bencana Geologi, 7(2), 79–88. (in Indonesian)

Susilo, A., Zulaikah, S., Pohan, A.F., Hasan, M.F.R., Hisyam, F., Rohmah, S., & Adhi, M.A., 2024. Vulnerability Index Assessment for Mapping Ground Movements Using the Microtremor Method as Geological Hazard Mitigation. Civil Engineering Journal, 10(5), 1616–1626. https://doi.org/10.28991/CEJ-2024-010-05-017.

Zhang, S., Tao, D., Xie, Q., Ma, Q., & Wang, F., 2021. Analysis of site amplification and nonlinear response based on ground motion records at MYGH10 station in Japan. Research Square preprint. https://doi.org/10.21203/rs.3.rs-1122308/v1.

Zulfiar, M.H., Tamin, T., Pribadi, K.S., & Irwan, I., 2014. Identification of dominant factors causing building vulnerability in earthquake-prone areas, West Sumatra Province. Semesta Teknika, 17(2), 116–125. (in Indonesian)

Manuscript received 9 October 2024;
Received in revised form 11 July 2025;
Accepted 25 September 2025
Available online 27 November 2026